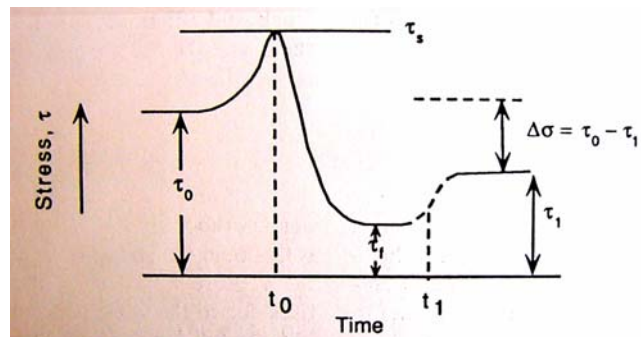


Earthquake Dynamics

Stress Behavior During Faulting



$$\Delta\sigma = \tau_0 - \tau_1 \quad \text{Stress Drop}$$

$$\bar{\sigma} = \frac{1}{2}(\tau_0 + \tau_1) \quad \text{Average Stress}$$

- Only the change in stress can be observed seismically – absolute stress cannot
- Stress drop in earthquakes typically ranges from 10-100 bars (1-10 MPa)
- Lithostatic stress is at least an order of magnitude larger

$$P = \rho gh = 2.67 \cdot 981 \cdot (10 \cdot 10^5) = 2600 \text{ bars}$$

Stress Drop

$$\Delta\sigma = C\mu\frac{\bar{u}}{L}$$

$$L = C\left(\frac{M_0}{\Delta\sigma}\right)^{1/3}$$

$$M_0 = \mu L^2 \bar{u}$$

$$f_c = \frac{1}{C}\left(\frac{\Delta\sigma}{M_0}\right)^{1/3} \beta$$

$$\Delta\sigma = C\frac{M_0}{L^3}$$

Equations for Stress Drop

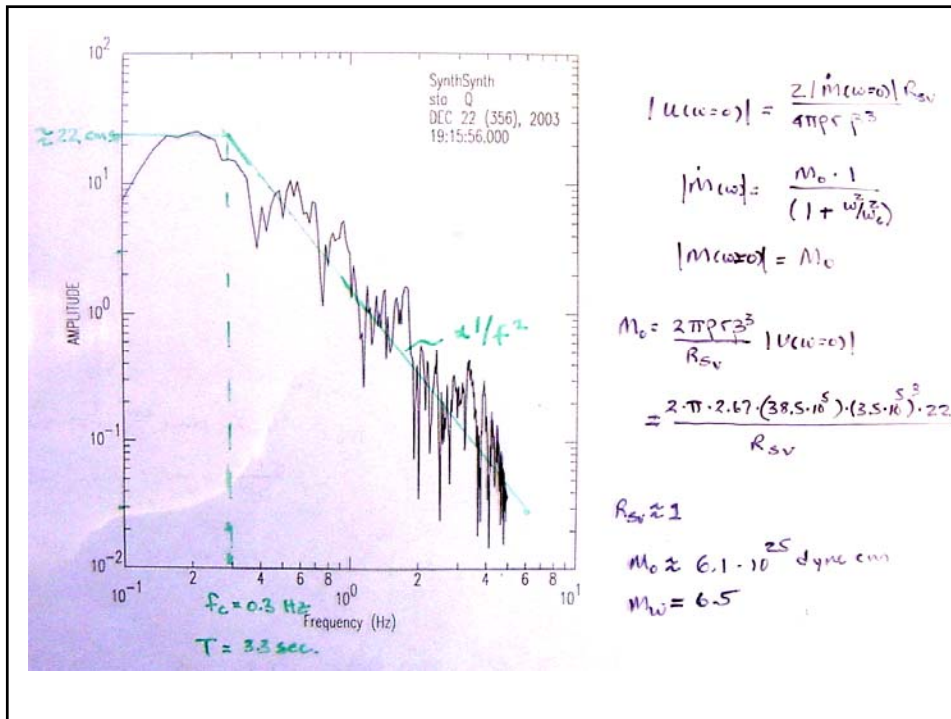
	Circular ($\lambda = \mu$)	Strike Slip	Dip Slip
Stress drop ($\Delta\sigma$)	$\frac{7\pi}{16} \mu \frac{(D)}{a}$	$\frac{2}{\pi} \mu \left(\frac{D}{w}\right)$	$\frac{4(\lambda + \mu)}{\pi(\lambda + 2\mu)} \mu \left(\frac{D}{w}\right)$
Strain energy ($\Delta W = S\sigma D$)	$\frac{16}{7\mu} a^3 \Delta\sigma \bar{\sigma}$	$\frac{\pi}{2\mu} w^2 L \Delta\sigma \bar{\sigma}$	$\frac{\pi(\lambda + 2\mu)}{4(\lambda + \mu)\mu} w^2 L \Delta\sigma \bar{\sigma}$
Moment ($M_s = \mu S D$)	$\frac{16}{7} \Delta\sigma a^3$	$\frac{\pi}{2} \Delta\sigma w^2 L$	$\frac{\pi(\lambda + 2\mu)}{4(\lambda + \mu)} \Delta\sigma w^2 L$

FIG. 1. Relations between stress drop, strain energy, offset, dimension, and moment for static cracks. Dimensions of the fault are a radius, L length, w width; initial stress is σ_0 ; final stress is σ_1 ; stress drop is $\Delta\sigma = \sigma_0 - \sigma_1$; average stress is $\bar{\sigma} = (\sigma_0 + \sigma_1)/2$; average dislocation is D .

$$\Delta\sigma = \frac{7 M_0}{16 a^3}$$

$$M_0 = \frac{2}{\pi} \mu (\pi a^2) \bar{\sigma}$$

What do we need to measure?



Estimation of Static Stress Drop & Radiated Energy for the San Simeon EQ.

since $\Delta\bar{\sigma} = \frac{7M_0}{16a^3}$ we will find the stress drop for an "equivalent" circular fault.

assuming that the radius is a function of the rupture speed and time we have...

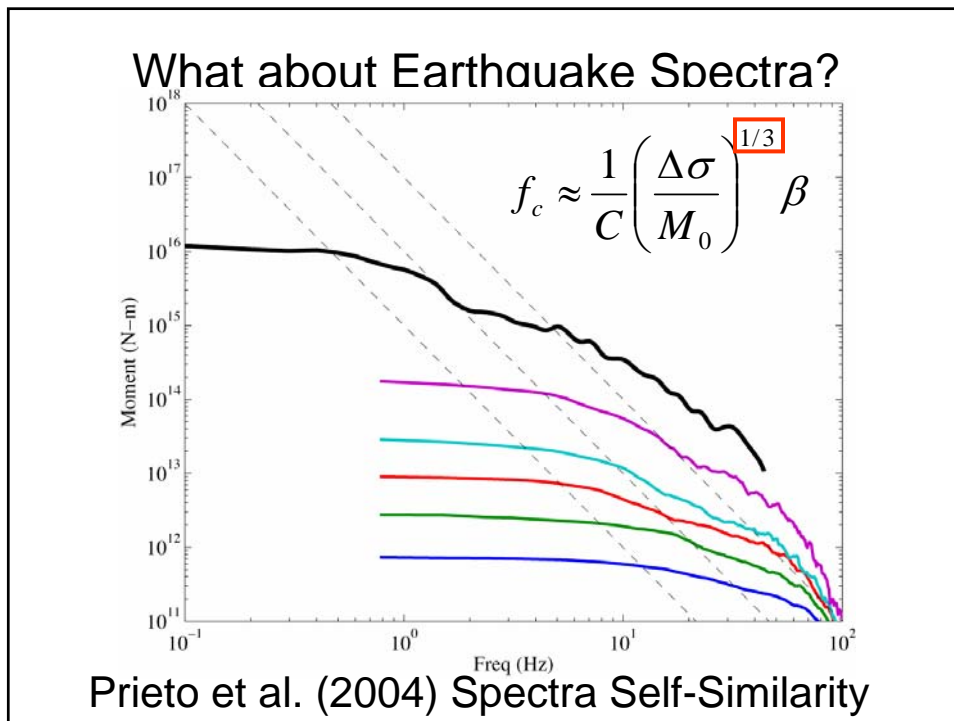
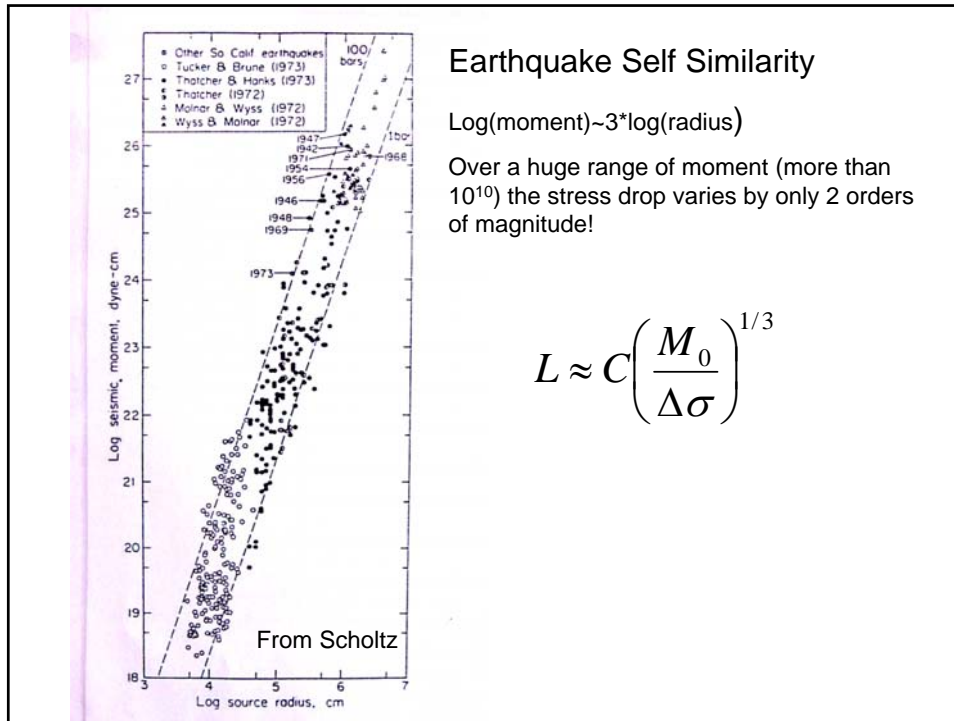
$$\begin{aligned} a &= v_r \cdot \tau \quad \text{since } v_r \approx \beta \\ &= \beta \tau = \beta / f_c \end{aligned}$$

then

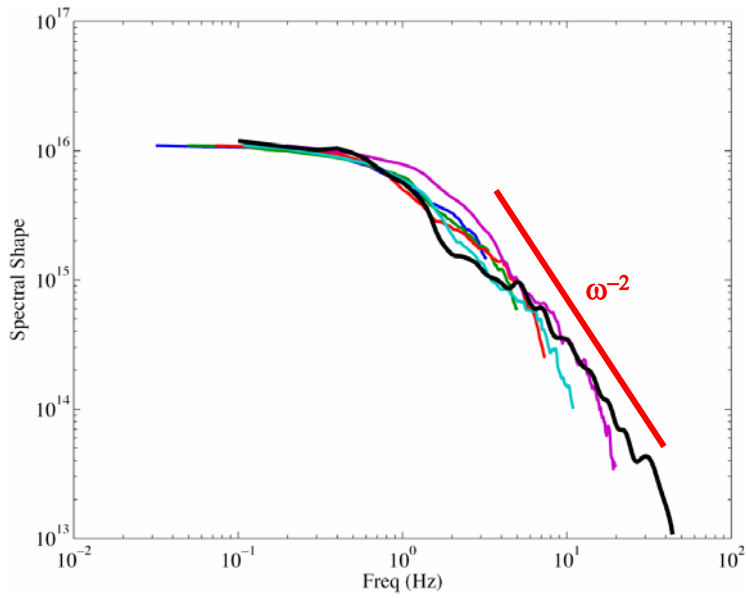
$$\begin{aligned} \Delta\bar{\sigma} &= \frac{7}{16} M_0 \left(\frac{f_c}{\beta} \right)^3 \\ &= \frac{7}{16} (6 \cdot 10^{25} \text{ dyne cm}) \frac{(0.3 \text{ s}^{-1})^3}{(3.5 \cdot 10^5 \text{ cm/s})^3} \\ &= 1.65 \cdot 10^7 \frac{\text{dyne}}{\text{cm}^2} = 16.5 \text{ bars} \end{aligned}$$

$$1 \text{ bar} = 10^6 \text{ dyne/cm}^2$$

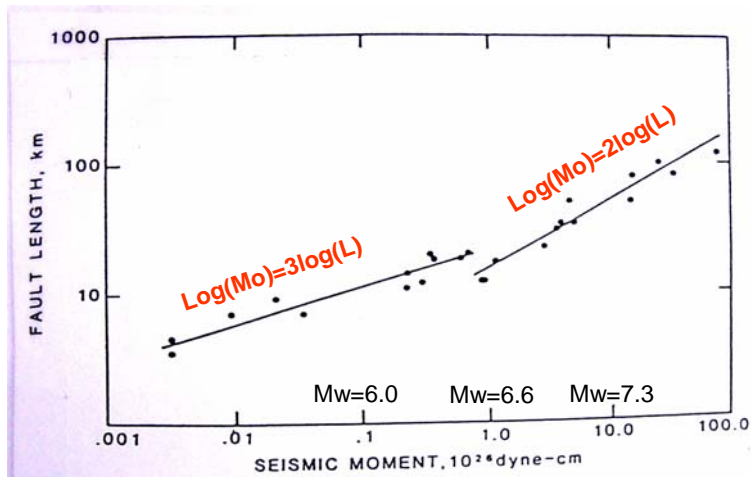
$$\begin{aligned} E_r &= \frac{(16.5 \cdot 10^6)}{2 \cdot 3 \cdot 10^{11}} \cdot 6 \cdot 10^{25} = 1.65 \cdot 10^{21} \text{ dyne cm} \\ &= 1.65 \cdot 10^{14} \text{ Joules} \end{aligned}$$



Prieto et al. (2004) Spectra Self-Similarity



A Break In Scaling



Modified from Scholtz

If L Grows Bigger than Seismogenic Thickness

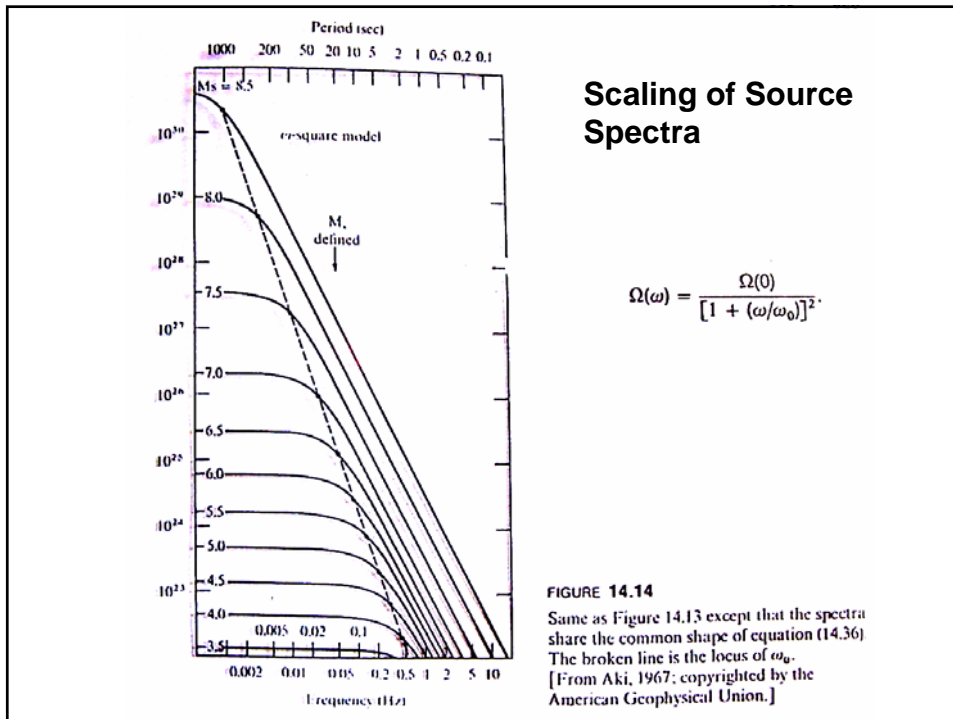
$$\Delta\sigma = C\mu\frac{\bar{u}}{L}$$

$$M_0 = \mu LW\bar{u}$$

$$\Delta\sigma = C\frac{M_0}{L^2W}$$

$$L = C\left(\frac{M_0}{\Delta\sigma W}\right)^{1/2}$$

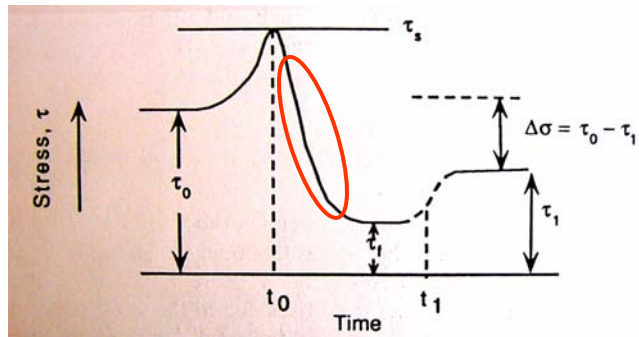
$$f_c = \frac{1}{C}\left(\frac{\Delta\sigma W}{M_0}\right)^{1/2}\beta$$



Scaling of Source Spectra

- How spectra change with moment
- How spectra change with stress drop

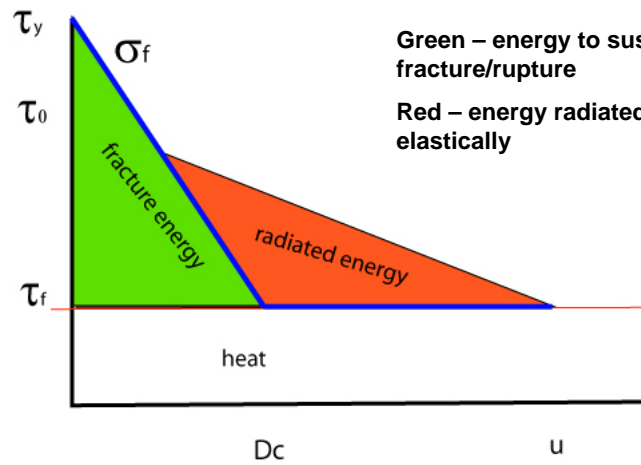
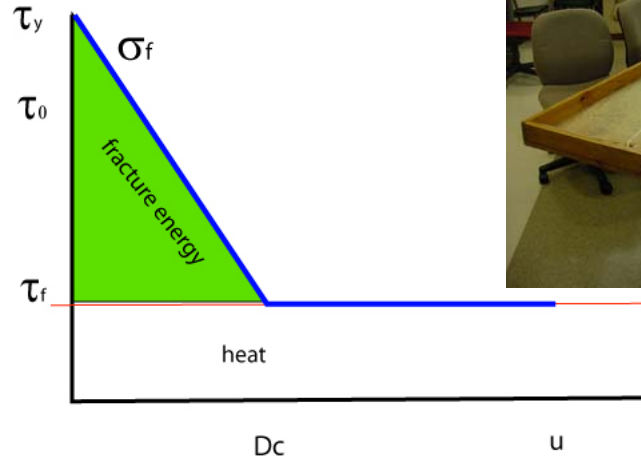
Stress Behavior During Faulting



$$\Delta\sigma = \tau_0 - \tau_1 \quad \text{Stress Drop}$$

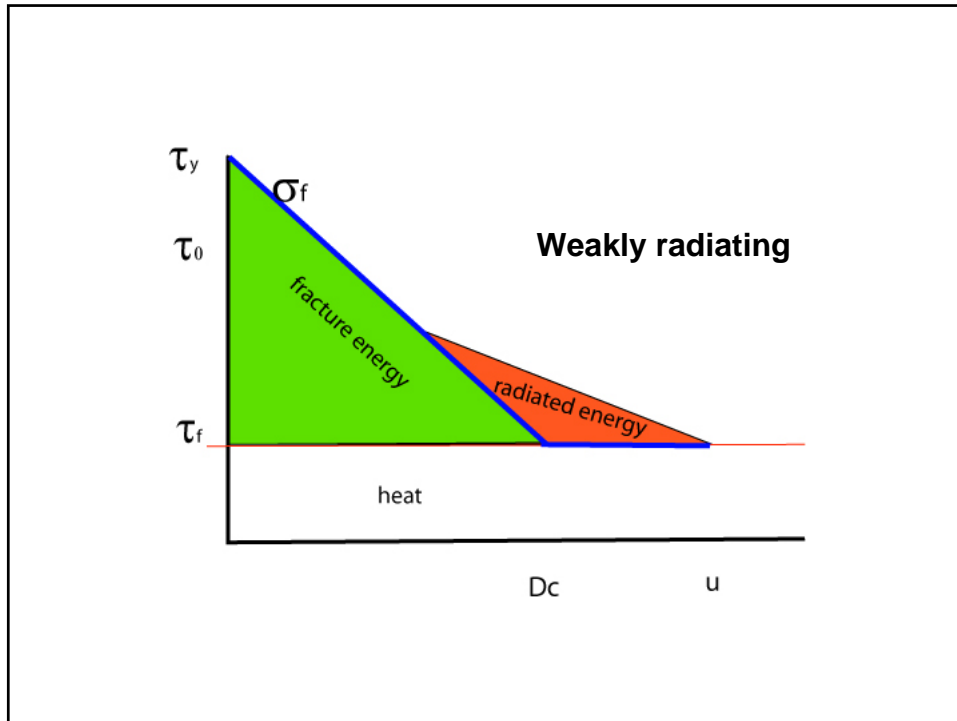
$$\bar{\sigma} = \frac{1}{2}(\tau_0 + \tau_1) \quad \text{Average Stress}$$

Slip Weaking Law



Green – energy to sustain fracture/rupture
Red – energy radiated elastically

Energy Budget



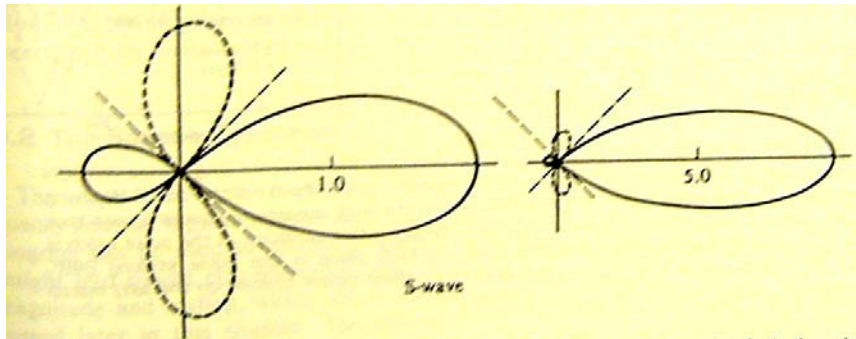
Radiated Energy

$$E_R = \bar{\sigma} u A = \frac{\bar{\sigma} M_0}{\mu} = \frac{\Delta \sigma M_0}{2\mu}$$

$$\log(E_R) = 1.5M + 11.8 \quad \text{Gutenberg}$$

$$E_R = c \int \dot{u}^2(t) dt = c \int \dot{u}^2(\omega) d\omega$$

Directivity & Radiation Patterns



$V_r/\beta=0.5$

$V_r/\beta=0.9$

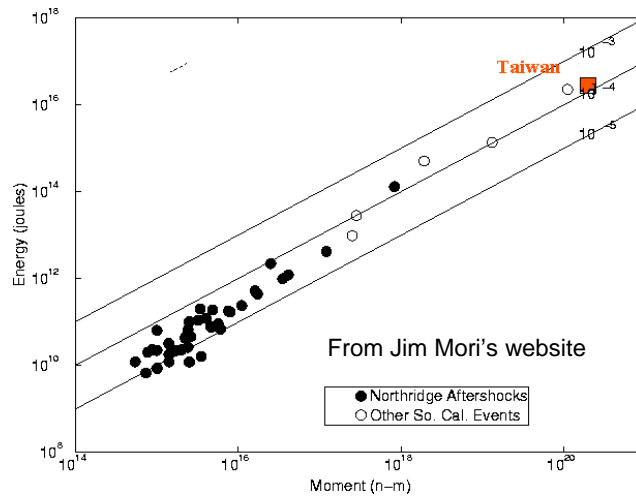
then

$$\begin{aligned}\Delta \bar{U} &= \frac{7}{16} M_0 \left(\frac{f_c}{\beta} \right)^3 \\ &= \frac{7}{16} (6 \cdot 10^{25} \text{ dyne cm}) \left(\frac{0.3 \text{ 1/s}}{3.5 \cdot 10^5 \text{ cm/s}} \right)^3 \\ &= 1.65 \cdot 10^7 \frac{\text{dyne}}{\text{cm}^2} = 16.5 \text{ bars}\end{aligned}$$

$$1 \text{ bar} = 10^6 \text{ dyne/cm}^2$$

$$\begin{aligned}E_r &= \frac{(16.5 \cdot 10^6)}{2 \cdot 3 \cdot 10^{11}} \cdot 6 \cdot 10^{25} = 1.65 \cdot 10^{21} \text{ dyne cm} \\ &= 1.65 \cdot 10^{14} \text{ Joules}\end{aligned}$$

Scaling of Radiated Energy?

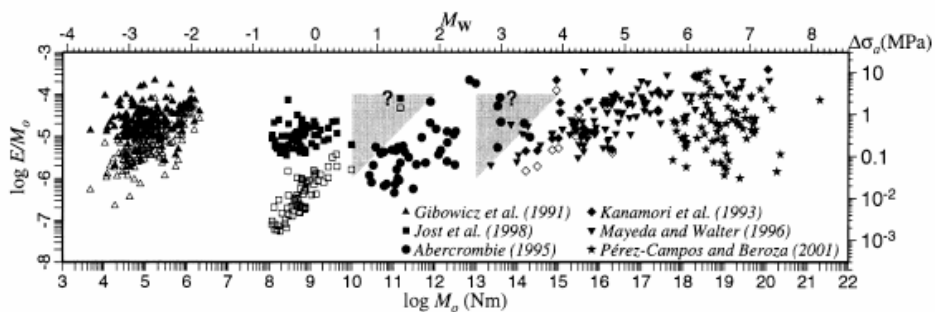


An increasing rate of radiated energy to seismic moment suggests different frictional properties of large earthquakes. Melting, thermal pressurization, and other lubrication mechanisms can reduce friction and thereby increase the ratio of energy to moment with increasing moment.

Scaling of Radiated Energy?

IDE AND BEROZA: DOES APPARENT STRESS VARY WITH EARTHQUAKE SIZE?

3351

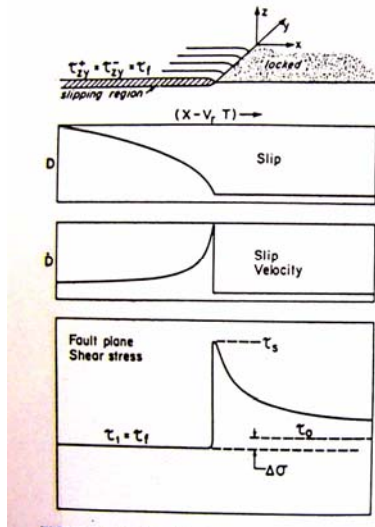


Accounting for limited recording bandwidth, and attenuations in published studies suggests a nearly constant ratio of radiated energy to moment (Ide and Beroza (2001).

The scaling of energy to moment is an active, passionately debated current research area.

Crack-like rupture

Slip rise time equivalent to total rupture time



Pulse-like rupture

Velocity dependent friction

Slip rise time much less than total rupture time

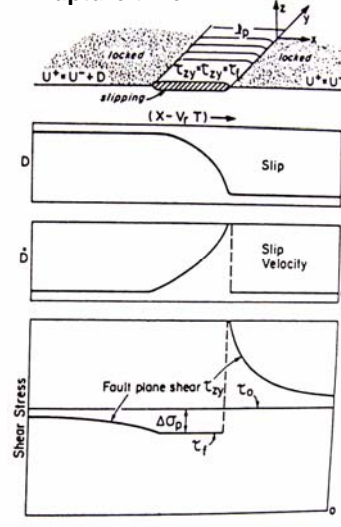


Fig. 4. Slip distribution (cm) for the $M=6.5$ 1979 Imperial Valley, CA, earthquake derived by Hartzell and Heaton (1983) from the simultaneous inversion of strong motion and teleseismic waveform data. The large dot denotes the hypocenter and the stippled region denotes the approximate region that is slipping at a particular instant in time.

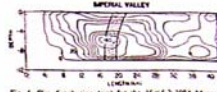


Fig. 5. Slip distribution (cm) for the $M=6.2$ 1984 Morgan Hill, CA, earthquake derived by Hartzell and Heaton (1984) from the inversion of strong motion waveform data. The large dot denotes the hypocenter and the stippled region denotes the approximate region that is slipping at a particular instant in time.

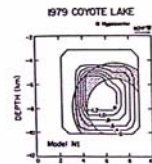


Fig. 7. Slip distribution (cm) for the $M=5.9$ 1979 Coyote Lake, CA, earthquake derived by Liu and Heineberger (1982) from modeling strong motion waveform data. The stippled region denotes the approximate region that is slipping at a particular instant in time.

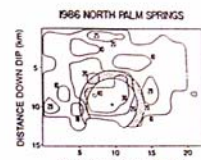


Fig. 4. Slip distribution (cm) for the $M=6.8$ 1986 North Palm Springs, CA, earthquake derived by Hartzell (1985) from the inversion of strong motion waveform data. The large dot denotes the hypocenter and the stippled region denotes the approximate region that is slipping at a particular instant in time.

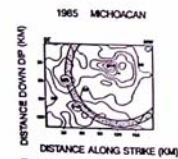


Fig. 1. Slip distribution (cm) for the $M=7.1$ 1982 Michoacan, Mexico, earthquake derived by Mendoza and Hartzell (1987) from the simultaneous inversion of teleseismic and strong motion waveform data. The large dot denotes the hypocenter and the stippled region denotes the approximate region that is slipping at a particular instant in time.

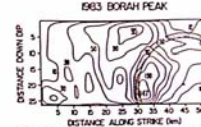


Fig. 3. Slip distribution (cm) for the $M=7.5$ 1982 Borah Peak, ID, earthquake derived by Mendoza and Hartzell (1987) from the inversion of long- and short-period teleseismic waveform data. The large dot denotes the hypocenter and the stippled region denotes the approximate region that is slipping at a particular instant in time.

Heaton and Heaton's (1990) analysis of kinematic rupture models indicates that only a small fraction of the fault is rupturing in a given instant.

The rise time from kinematic models represents a maximum value

Average Slip Velocity

$$\Delta\sigma \approx C\mu \frac{\bar{u}}{L}$$

$$\bar{u} \approx \frac{\Delta\sigma}{C\mu} L = \frac{\Delta\sigma}{C\mu} \beta t$$

$$\dot{\bar{u}} \approx \frac{\Delta\sigma}{C\mu} \beta \approx \frac{60 \cdot 10^6}{3.5 \cdot 10^{11}} * 3.5 \cdot 10^5 \approx 60 \frac{cm}{s}$$



Fig. 4. Slip distribution (cm) for the $M=6.5$ 1979 Imperial Valley, CA, earthquake derived by Hartzell and Heaton (1983) from the simultaneous inversion of strong motion and teleseismic waveform data. The large dot denotes the hypocenter and the stippled region denotes the approximate region that is slipping at a particular instant in time.

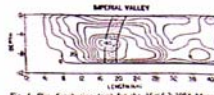


Fig. 5. Slip distribution (cm) for the $M=6.2$ 1984 Morgan Hill, CA, earthquake derived by Hartzell and Heaton (1984) from the inversion of strong motion waveform data. The large dot denotes the hypocenter and the stippled region denotes the approximate region that is slipping at a particular instant in time.

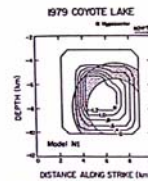


Fig. 7. Slip distribution (cm) for the $M=5.9$ 1979 Coyote Lake, CA, earthquake derived by Liu and Heineberger (1982) from modeling strong motion waveform data. The stippled region denotes the approximate region that is slipping at a particular instant in time.

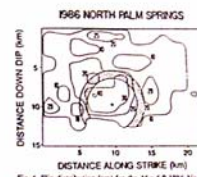


Fig. 4. Slip distribution (cm) for the $M=6.0$ 1986 North Palm Springs, CA, earthquake derived by Hartzell (1989) from the inversion of strong motion waveform data. The large dot denotes the hypocenter and the stippled region denotes the approximate region that is slipping at a particular instant in time.

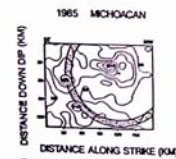


Fig. 1. Slip distribution (cm) for the $M=7.1$ 1982 Michoacan, Mexico, earthquake derived by Mendoza and Hartzell (1987) from the simultaneous inversion of teleseismic and strong motion waveform data. The large dot denotes the hypocenter and the stippled region denotes the approximate region that is slipping at a particular instant in time.

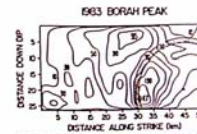
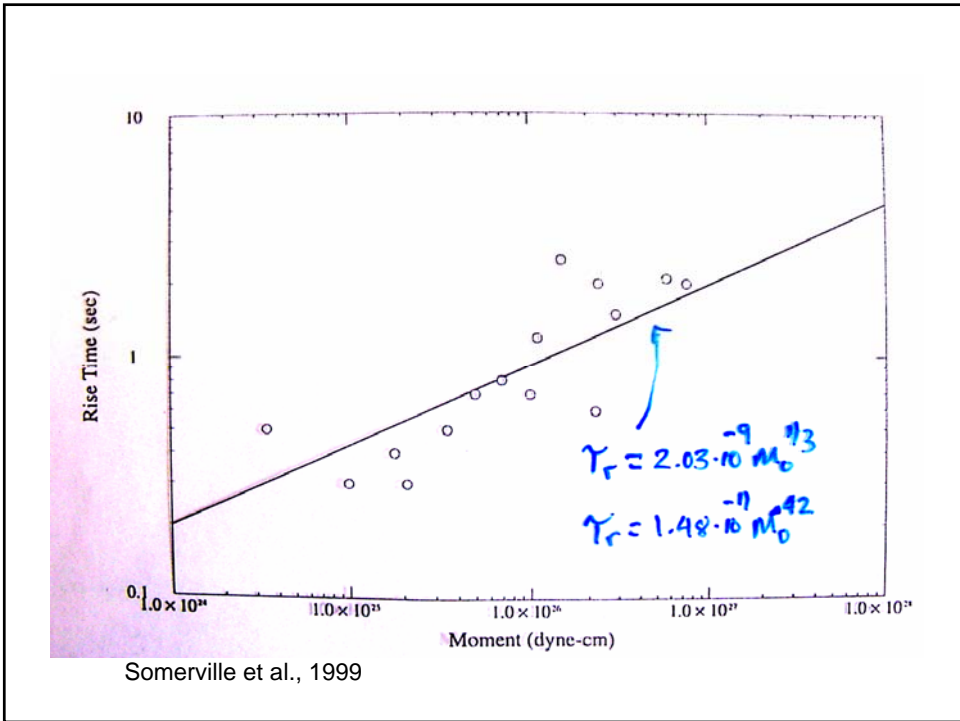
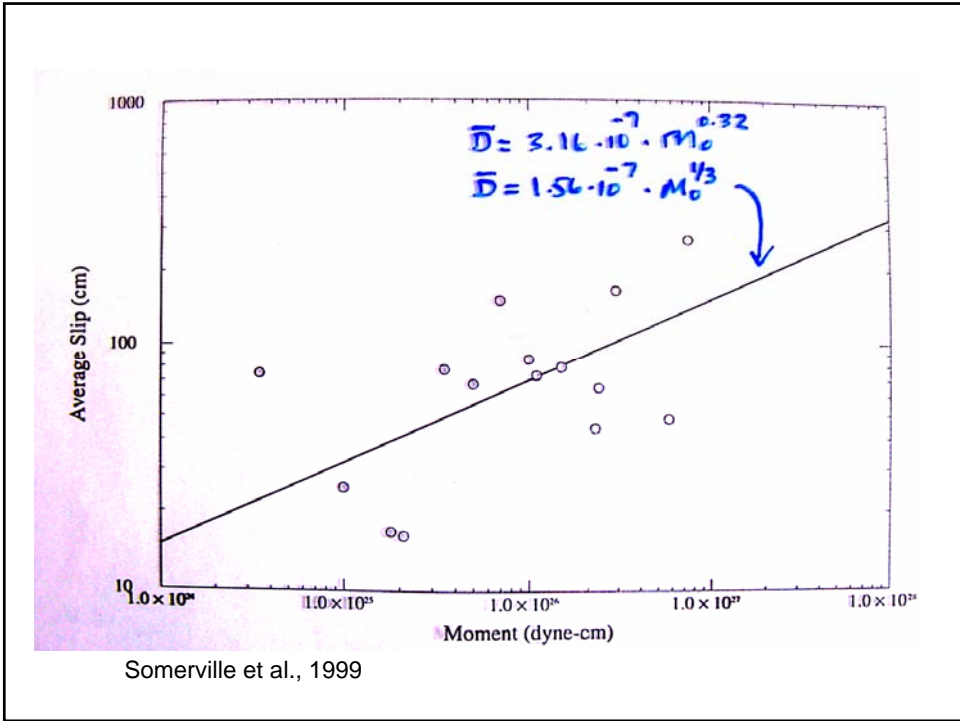


Fig. 3. Slip distribution (cm) for the $M=7.5$ 1982 Borah Peak, ID, earthquake derived by Mendoza and Hartzell (1987) from the inversion of long- and short-period teleseismic waveform data. The large dot denotes the hypocenter and the stippled region denotes the approximate region that is slipping at a particular instant in time.

Heaton and Heaton's (1990) analysis of kinematic rupture models indicates that only a small fraction of the fault is rupturing in a given instant.

The rise time from kinematic models represents a maximum value

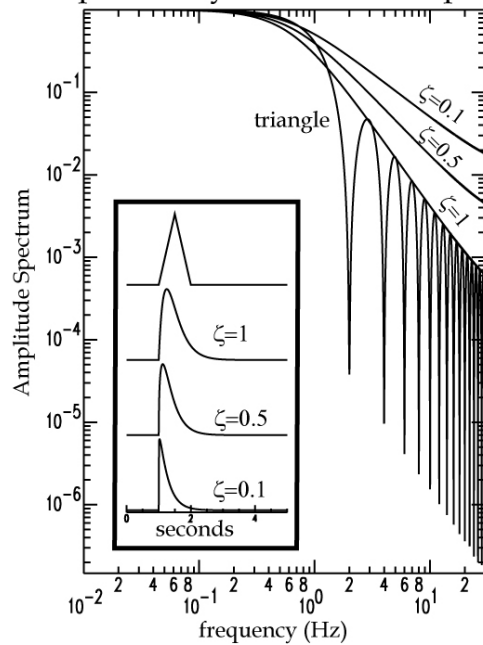


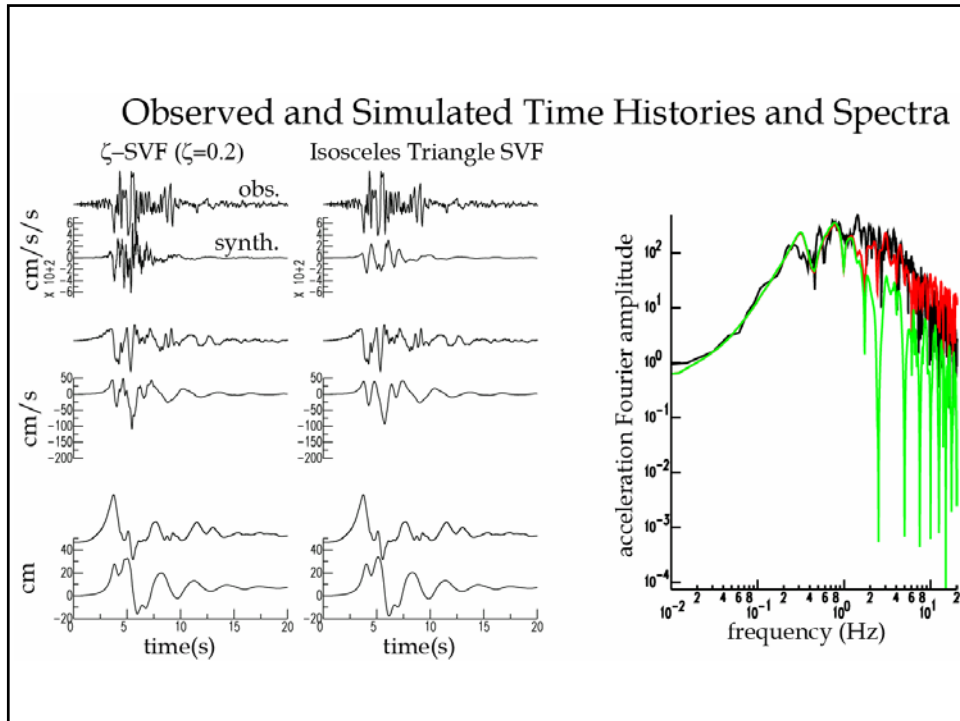
Average Slip Velocity from Kinematic Models

$$\dot{\bar{u}} = \frac{\bar{D}}{\tau_R} = \frac{1.56 \cdot 10^{-7}}{2.03 \cdot 10^{-9}} \frac{M_0^{1/3}}{M_0^{1/3}} \approx 77 \frac{cm}{s}$$

Based on Somerville et al., 1999

Slip Velocity Functions & Spectra





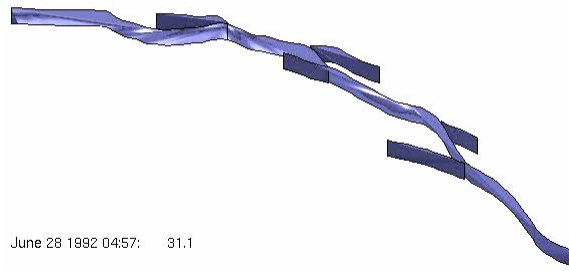
Dynamic Rupture Model for the Landers Earthquake – courtesy of Kim Olsen (SDSU)



Rupture is governed by initial and yield stress distribution, and a constitutive slip weakening friction law.

Heterogeneous slip and slip velocity are calculated.

Another View – Pwaves (green), Swaves (magenta)



TerraShake Simulation

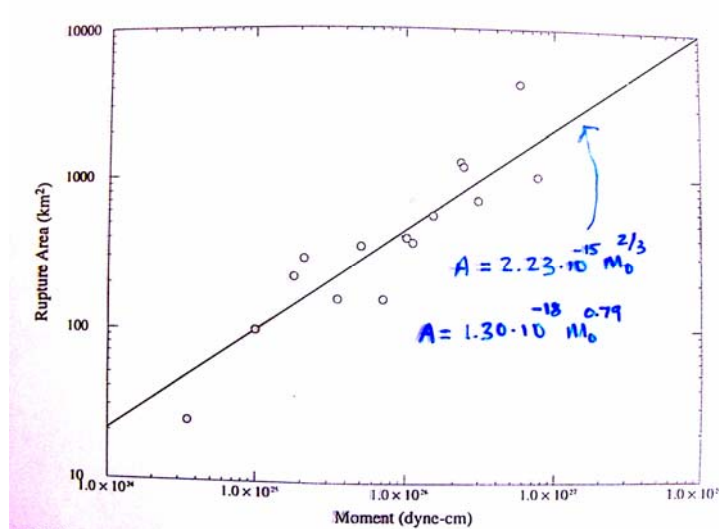
[Quick time](#)

Check out:

<http://ucsdnews.ucsd.edu/newsrel/general/terrashake.asp>

<http://visservices.sdsc.edu/projects/scec/terashake/2.1/>

Rupture Area Scaling



Somerville et al., 1999

Summary of Scaling

- As earthquakes grow larger the following increase:
 - Fault length, width, and area
 - Seismic moment & Radiated Energy
 - Rupture duration & average slip
- & the following stay the same:
 - Average stress drop
 - Average slip velocity
 - Rupture velocity
 - Ratio of Radiated Energy to Seismic Moment